REPORT DOCUMENTATION PAGE

Form Approved
OMB NO. 0704-0188

~~ARO/DARPA Final AMXRO-ICA 40067-EL DAAD19-99-1-0154~~

1. AGENCY USE ONLY (Leave Blank)	2. REPORT DATE	3. REPORT TYPE AND DATES COVERED
	March 31, 2004	~~Final. Jan. 1, 2003 – Dec. 31, 2003~~ 15 Apr 99 – 15 oct 03

4. TITLE AND SUBTITLE
Inverse Nottingham Effects Cooling of Semiconductors with Resonant Tunneling

5. FUNDING NUMBERS
AMXRO-ICA 40067-EL
~~DAAD19-99-0154~~
DAAD19-99-1-0154

6. AUTHOR(S)
Raphael Tsu

7. PERFORMING ORGANIZATION NAME(S) AND ADDRESS(ES)
UNC-Charlotte, Charlotte NC 28223

8. PERFORMING ORGANIZATION REPORT NUMBER

9. SPONSORING / MONITORING AGENCY NAME(S) AND ADDRESS(ES)
U. S. Army Research Office
P.O. Box 12211
Research Triangle Park, NC 27709-2211

10. SPONSORING / MONITORING AGENCY REPORT NUMBER
40067-EL
.1

11. SUPPLEMENTARY NOTES
The views, opinions and/or findings contained in this report are those of the author(s) and should not be construed as an official Department of the Army position, policy or decision, unless so designated by other documentation.

12 a. DISTRIBUTION / AVAILABILITY STATEMENT
Approved for public release; distribution unlimited.

12 b. DISTRIBUTION CODE

13. ABSTRACT (Maximum 200 words)
Heat removal by Inverse Nottingham Effect (INE) is a new concept utilizing hot electrons emitted from the semiconductor surface into the vacuum via field emission. The replenishment of hot electrons in the semiconductor as a result of re-establishment of thermal equilibrium constitutes cooling. To avoid heating from current crowding, tips are replaced by a double barrier resonant tunneling structure (DBRT) at the surface of a semiconductor to allow efficient field emission via resonant tunneling. We recognized that the most important step is to achieve high emission from the semiconductor into the vacuum. A double barrier structure with $Ga_{.5}$ $AL_{.5}$ N as barrier material with GaN well is designed and chosen for the desired high emission. A CVD structure grown by Prof. A. Khan, on SiC substrate, taken to University Lyon to be measured by Prof. Binh, resulted in a breakthrough for field emission, with a threshold field of 50 V / μm, with stable FE current densities of $3x10^{-2}A/cm^2$. (V. Semet, V.Binh, J, Zhang, J.Yang, A.Khan and R. Tsu, APL 84, 1937, 2004). Although we have not succeeded in cooling due to problems created by radiation back from the anode, this breakthrough in field emission is an important by-product of our research which can benefit various field, principally vacuum electronics, such as cold cathode for traveling wave tubes. In fact, the measured exceeded the calculated because we did not realize that the bulk of the high emission came from the effective lowering of the work function at the surface created by space charge in the quantum state.

14. SUBJECT TERMS	15. NUMBER OF PAGES 23
	16. PRICE CODE

17. SECURITY CLASSIFICATION OR REPORT	18. SECURITY CLASSIFICATION ON THIS PAGE	19. SECURITY CLASSIFICATION OF ABSTRACT	20. LIMITATION OF ABSTRACT
UNCLASSIFIED	UNCLASSIFIED	UNCLASSIFIED	**UL**

20040514 026

REPORT DOCUMENTATION PAGE (SF298)

(1) List of Publications related to INE

R. Tsu and R.F.Greene, "Inverse Nottingham Effest Cooling in Semiconductors", *Electrochem and Solid-State Lett.*, **2** (1999) 645-647 (1999)

Cooling by Field Emission with Resonant Tunneling : Design Parameters, R. Tsu, Cold Cathode, ECS Proc. Vol. **2000-28**, 91 (2001)

Cooling by Inverse Nottingham Effect with Resonant Tunneling , Y. Yu, R.F.Greene, and R. Tsu, International J. High Speed Electronics and Systems **12**, 1083-1100 (2002)

Cooling by Inverse Nottingham Effect with Resonant Tunneling , Y. Yu, R.F.Greene, and R. Tsu, Adv. Semiconductor Heterostructures, Eds. M. Dutta and M. Stroscio (World Sci. 2003, Singapore) p.145

Electron emission through a multilayer planar nanostructured Solid-state field-controlled emitter, V. Semet, V.Binh, J, Zhang, J.Yang, A.Khan and R. Tsu, Appl. Phys. Lett. **84**, 1937 (2004)

(2) Scientific personnel supported by this project and degrees awarded or pending during this reporting period:

Scientific personnel supported :

a. UNCC: PI, R. Tsu, Co-PI R.F.Greene retired

Students:

Yuan Yu	PhD Candidate (1/2)
Jinwen Zhu	PhD Candidate (1/2)

Postdoctoral Fellow :

Osmond Gurdal	1/01/2001– 8/31/2001 (¼)

b. Sarnoff : Heinz Busta until June 2001, taken over by Jia Ming Chen , (609) 734-2101

c. State U. of New York-Stony Brook PI, Kostantin K. Likharev, with assistance from Wiley P. Kirk (Texas A & M University)

d. NC State Univ. PI: J. Cuomo until Dec. 2002, taken over by Robert F. Davis, (919) 515-2867 assisted by Postdoctoral fellow Sven Einfeldt

e. SVT Associates, Inc. PI: Peter Chow, SVT Assoc. Inc.

3. Progress and Accomplishments

Since the most completely version is in the publication listed in the 2nd item in (1), most of the contents will be repeated here.

The Inverse Nottingham Effect (INE) cooling involves emission of electrons above the Fermi level into the vacuum. Our scheme involves the use of a Double Barrier Resonant Tunneling (DBRT) section positioned between the surface and the vacuum for a much increased emission, and to provide energy selectivity for assuring cooling, without surface structuring such as tips and ridges leading to current crowding and additional heating. Unlike resonant tunneling from contact-to-contact, where barrier heights and thickness are controlled by the choice of heterojunctions, the work function at the surface dictates the barrier height for tunneling into the vacuum. The calculated field emission via resonant tunneling gives at least two orders of magnitude greater than without resonance, however, without work function lowering, the large gain happens at fairly high field. The use of resonance to enhance cooling by INE results in an important byproduct, an efficient cold-cathode field emitter for vacuum electronics.

Introduction

The original Nottingham effect dealt with the additional thermal effects beyond the non-ohmic behavior field emission from metal tips.[1] The Inverse Nottingham Effect (INE) cooling involves emission of electrons above the Fermi level into the vacuum.[2-4] Our scheme involves the use of a Double Barrier Resonant Tunneling (DBRT) section positioned between the surface and the vacuum for a much increased emission, and to provide energy selectivity for assuring cooling, without surface structuring such as tips and ridges leading to current crowding and additional heating. Two approaches appeared: (1) The G-T, Greene-Tsu, scheme consists of inserting a double barrier resonant tunneling section, [5-7] between the surface of the semiconductor to be cooled and the vacuum. (2) The K-L, Korotkov-Likharev, scheme consists of a step inserted between the semiconductor and the vacuum. Under the application of a high electric field, the step forms a triangular quantum well for resonance tunneling.[4] The G-T scheme offers better flexibility in design possibility for optimizing cooling while keeping the electric field at the surface to a 'safe limit'. The K-L scheme is simple, however, because the step is a barrier material, usually formed by alloying resulting in lower mobility and hence lower efficiency. There is a basic principle of symmetry when resonant tunneling is involved. The maximum transmission at resonance requires a symmetrical structure. It is easy to understand the need for a symmetrical structure. Imagine that a resonant cavity for photons, the Fabry-Perot interferometer

having one surface reflectivity much larger than the other, then it is not possible to build up the field from coherent interference without a symmetrical structure. In DBRT, if one designs a symmetrical structure without a bias voltage applied, the applied voltage will destroy the symmetry. Therefore it is important to design the barrier structures as symmetrical as possible at the operating resonant condition. Thus it is necessary to design a symmetrical potential profile at the operating voltage.[7] Unlike resonant tunneling from contact-to-contact, where barrier heights and thickness are controlled by the choice of heterojunctions. For tunneling into the vacuum, the work function at the surface dictates the barrier height. And this is the difficulty in optimizing tunneling into the vacuum via DBRT, because typically the first barrier height is ~ few tenth of eV above the quantum well, but the 2nd barrier, is determined by the work function, usually several eVs above the quantum well. One may assume that a very thick 1st barrier can match the high work function of the 2nd barrier. In principle it is possible, however, the quantum state with thick barriers, instead of a resonant state, is practically an eigenstate, having almost no energy width to support a large tunneling current. Therefore, we have concluded that the best way is to search for a 2nd barrier with very low work-function.[7] For this reason, under the HERETIC DARPA/ARO program, we have been pushing the structure with III-nitrides. In view of the conflicting claims of negative electron affinity for AlGaN with [Al] / [Ga] over 60%, and also it is doubtful that such material may have good mobility, we calculated cases where we do not need the low work function. Basically, we know that resonant tunneling can enhance field emission. We want to see how much gain over the usual Fowler-Nordheim tunneling. It is indeed encouraging that the calculated field emission via resonant tunneling is several orders of magnitude above the F-N tunneling at a surface field of several 10^7 V/cm. And if we consider a surface field of up to ~ $2x10^7$ V/cm, it is 2-4 orders of magnitude higher. For cooling, it is important to extract the emission current with the Pierce-electrode,[3-8] which is difficult to implement, so that some of the power at the anode can be recovered as in traveling-wave tube designs.[8] Removing the heat at the anode is identical to removing the heat from the heat exchanger in any air conditioner. Even if all these practical problems cannot be overcome, there is a huge byproduct. Field emission with resonance results in an efficient cold-cathode field emitter for vacuum electronics, which is particularly important in high power TWT!

Background

Originally G-T scheme targeted the use of a p-type semiconductor to produce surface inversion as in the MOSFET to pull electrons above the Fermi level into the vacuum, [2] while the K-L scheme targeted the use of n-type.[4] We exclude the usual approach of surface structuring such as tips and ridges [9], because tips result in current crowding which leads to heating and the problem of robustness. This is the main reason why we decided on the use of DBRT to enhance field emission into the vacuum. For the convenience of the reader, the original G-T scheme for p-doped semiconductors method in Fig.1 of Ref. 2 is shown below as Fig. 1. It was shown that the average energy per electron above the Fermi level at the surface representing cooling is

$$< E - E_F > = A^{-1} [1.5\, k_B\, T + (E_{co} - E_F)] \quad , \tag{1}$$

in which A^{-1} term represents a reduction factor due to the presence of tunneling upsetting the balance between generation and recombination at thermal equilibrium.[2] Also for the convenience of the reader, the K-L scheme taken from Ref. 4 is reproduced in Fig. 2.

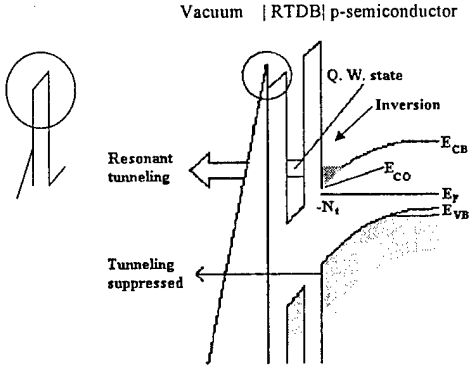

Fig.1 G-T (Greene-Tsu) scheme: Band profile of p-doped inversion layer under high electric field with tunneling into the vacuum via a DBRT structure. Also shown is trapping level at the interface, N_t, to be incorporated for increased replenishment of electrons pulled out into the vacuum.

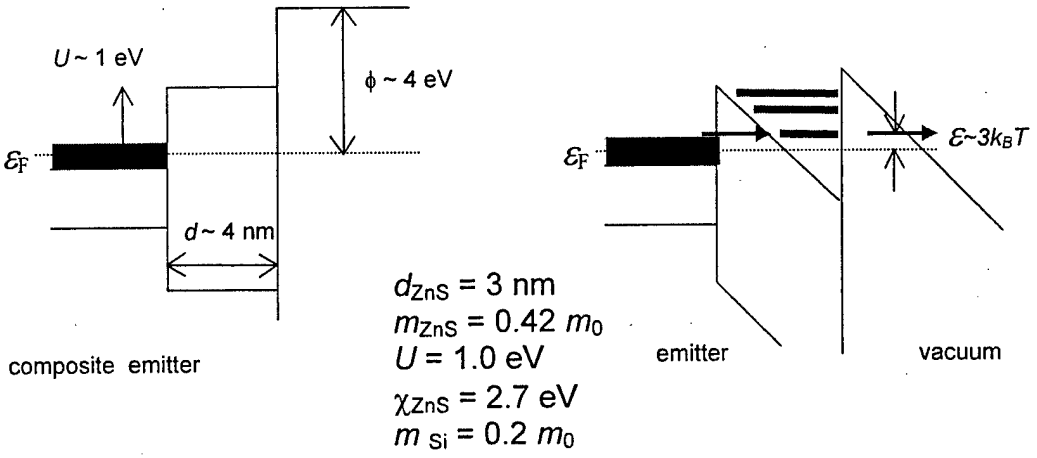

Fig.2 Band profile of the proposed emitter (a) no field, (b) with field. Horizontal lines in (b) show quantized sub-bands. Arrows show RT via the sub-bands. The lowest sub-band is placed at few k_BT above the Fermi level so that cooling occurs with removal of hot electrons of the emitter. Taken from Ref. 4.

Figure 2 of Ref. 7 that was missing.[7] It is reproduced as Fig. 3, showing without NEA (negative electron affinity), the 2nd barrier, the one next to the vacuum is so much thicker except under extremely high field, so that tunneling current is quite small as in (c).

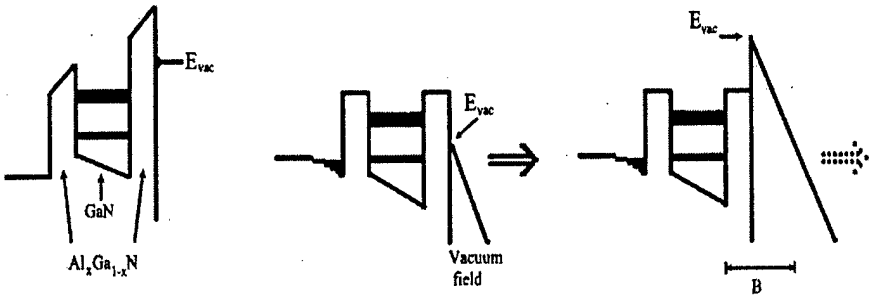

(a) (b) (c)

Fig 3: Three cases: (a) no applied voltage with NEA (negative electron affinity), (b) with applied voltage and NEA, and (c) same as (b) but without NEA, resulting in a large barrier marked as B; depending on the value of the applied voltage, the tunneling current into the vacuum is generally substantially reduced.

Whenever one barrier is much thicker than the other, the transmission coefficient is much reduced. As mentioned that the restoration of symmetry is key to the success of high gain at resonance in a DBRT structure, the transmission T and the maximum T, T_M presented in Ref. 7 are repeated here especially, due to printer's error, the figures were missing in Ref. 7. The reflectivity and phase shift of a single barrier are, [7]

$$R = (k^2+\alpha^2)^2 / [(k^2+\alpha^2)^2 + 4\,k^2\,\alpha^2\,F^2], \tag{2}$$

$$\phi = \tan^{-1}[2k\alpha F / (\alpha^2 - k^2)], \tag{3}$$

in which $\alpha^2 = \alpha_o^2 - k^2$, and $F = (1+e^{-2\alpha b}) / (1-e^{-2\alpha b})$, and $k^2 = 2m^*E / \hbar^2$, $\alpha_o^2 = 2m^*V_o / \hbar^2$, where V_o and b being the barrier height and width respectively. The transmission, T for well-width w is

$$T = T_1T_2 / [(1 - R_1)(1 - R_2) / (1 + R_1R_2 - 2(R_1R_2)^{1/2}\cos\Phi], \tag{4}$$

in which $\Phi = \phi_1 + \phi_2 + 2kw$. At resonance $\Phi = 2n\pi$, so that the maximum T is

$$T_M = T_1T_2 / [(1 - R_1)(1 - R_2) / (1 + (R_1R_2)^{1/2})]. \tag{5}$$

The calculated T_M is shown in Fig. 4 for various R_1 and R_2. Note that near unity T_M only occurs for $R_1 \sim R_2$. This is because unity T_M is obtained when the two reflectivities are equal for

maximum interference. As long as the structure is symmetrical, the transmission at resonance is always unity. Whenever one of the R_1 and R_2 is high, the other R must also be high to give a large T_M. For relatively low value of the reflectivity R, Q (Q is the quality factor of a resonating system defined by number of cycles a photon is confined before it decays to 1/ e of the initial value.) is low, and it does not take many traversals to produce a relatively high transmission. This is why we need thin barriers to produce high throughput. Since thin barrier needs low work function or NEA, III-nitrides seems to be the best choice at this point.

Figures 4 is really very important for optimizing the design of RTDs, but for RTFE, resonant tunneling field emission, the vacuum level is fixed by the work function, so that there is not much one can do about it. Optimization amounts to picking the right materials for the construction of the DBRT structure.

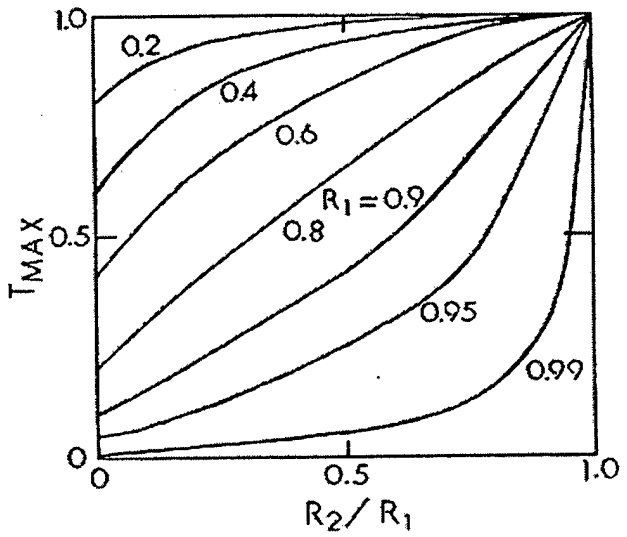

Fig. 4: T_M vs. the ratio R_2 / R_1 for various R_1. R_1 and R_2 are the reflectivity at the first- and second-barrier. Note that for $R_1 > 0.95$, T_M is only significant for $R_2/R_1 > 0.9$.

Direct computations for the tunneling current into the vacuum at resonance have been performed in this work. We found that the estimate for the thermal current for cooling of ~ 300 – 2000 W/cm^2 in Ref. 2, is too optimistic because in the previous estimate, the difference in the effective mass in the semiconductor and the free electron mass in the vacuum was not accounted for.

Computation of the RTFE

We have undertaken the direct computation of RTFE, resonant tunneling field emission, for n-type semiconductors with the barrier structures. Although we have stated several times that III- nitrides appear to be the most promising materials, we selected silicon for the calculation because as we shall see that we are far from obtaining practical design optimization partly

because resonant tunneling into the vacuum is far more complex than resonant tunneling from contact-to-contact.[5,6] We want to establish some rules governing high emission at a given electric field with the available material parameters. We start with the Tsu-Esaki approach[5] by integrating the transmission T given by the matrix relating the input at the left contact to the output at the right contact with the appropriate distribution and density of states functions for the total tunneling current density, the sum of j_{lr}, from left to right; and j_{rl}, from right to left, or

$$j_T = \frac{emk_BT}{2\pi^2\hbar^3}\int_0^\infty |T|^2 \ln\left(\frac{1+e^{(E_f-E_l)/k_BT}}{1+e^{(E_f-E_l-eV_a)/k_BT}}\right)\sqrt{\frac{E_l+eV_a}{E_l}}dE_l . \qquad (6)$$

Eq. (6) contains an extra term, under the square root, a correction term added in by Coon and Lieu.[10] This correction term is not so important in tunneling from contact-to-contact, but significant for tunneling from contact-to-vacuum where V_a may be quite large. Before we present cases of interest, let us define some terms useful for the remaining of this article. For emission to into the vacuum useful as a cold cathode, we need the total current j_T defined by an integration for E = 0 to ∞. For cooling, because we only remove the hot electrons, the current j_H is defined by an integration for E = E_F to ∞. Fig. 6 gives the comparison of the transmission coefficients of a structure, 5,5,7nm (the 1st barrier width, b, of 5nm, and quantum well width w of 5nm, and a vacuum barrier, the 2nd barrier of w = 7nm), and one without resonant tunneling having only the 2nd barrier of 7nm, the F-N tunneling. For better visualization, portion of Fig. 6 is plotted in linear scale shown in Fig. 7.

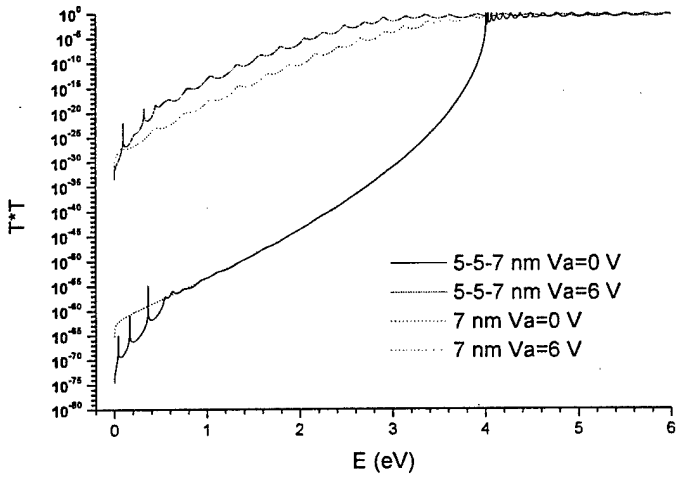

Fig. 6 Transmission vs. energy in eV with and without applied voltage V_a = 6 V corresponding to an electric field in the vacuum of 7.5x10^6 V/cm. 1st Barrier height = 0.5eV and 2nd Barrier height (vacuum side) = 4 eV

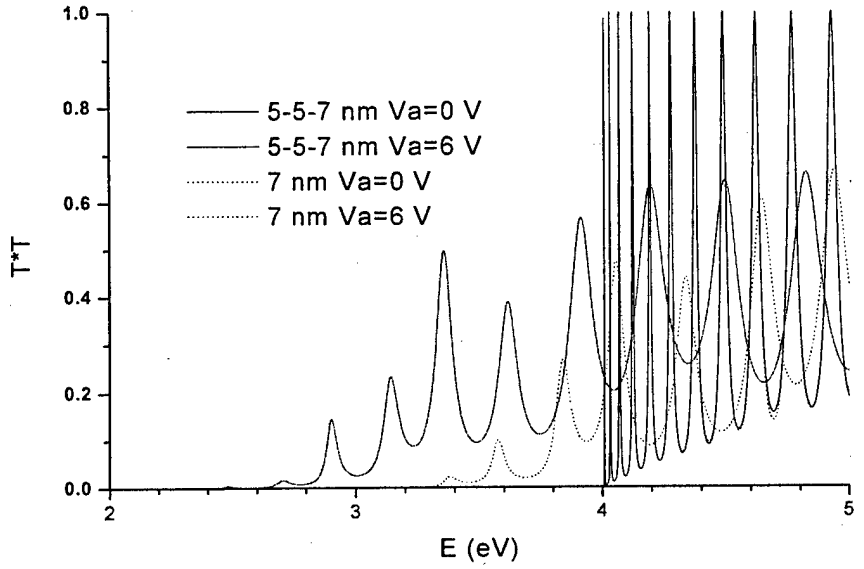

Fig.7 Transmission vs. energy with linear plot in the range of interest where T*T is large.

It is important that we discuss these two figures because the transmission is rather different from the conventional tunneling from contact-to-contact. Take, for example, the 5-5-7 case, the three peaks near E ~ 0 represent the resonance via the quantum well states. The peak values are so small because the structure is very asymmetrical due to the high 2nd barrier of 4 eV. In fact we thought that the computation was incorrect because we failed to find the resonant tunneling peaks first. After realizing that the value of these peaks may be so small that we missed them, we proceeded to look for them, and we found them as shown in Fig. 6. For E > 0.5 eV, there are small structures due to interference just above the 0.5eV of the 1st barrier height. There are no substantial resonant states until the energy is above the vacuum level, at E > 4 eV. The large oscillation of T*T between 0 and 1 comes from resonant states in the vacuum due to the vacuum barrier. This point is not too familiar to most although several years ago similar phenomena were treated regarding the physics of 'Quantum Step'. [11] In fact these resonant states in the vacuum can be calculated very simply from $k_n = n\pi / B$, with B being the distance between the surface of the semiconductor and the anode placement in the vacuum. With an applied +V with respect to the cathode, T*T shifts to the left. This shift is same as resonant tunneling from contact-to-contact. For a symmetrical structure, the spectrum is shifted by an amount in energy very close to V/2. Why is the magnitude of the oscillations so huge? What is happening is the fact that at higher energy, the 1st barrier and the well region play almost no role. The bulk of the oscillation is due to the vacuum barrier. The discontinuity of the barrier is further augmented by the difference of the effective mass in the semiconductor, and free electron mass in the vacuum. These oscillations are nearly the same for the case shown in dotted having only the vacuum barrier. Figure 7 shows a linear plot to give a better feeling what is happening. Note that as the applied voltage increases, these large oscillations of T*T move toward the origin as

discussed. When they pass the Fermi level of the left contact, substantial tunneling current appears. Again we emphasize that it only occurs at high electric field, > 10^7 V/cm. This type of oscillation of resonant tunneling via the quantized vacuum state cannot be obtained by the use of WKB perturbation usually used for computing tunneling. In fact Mimura et. al. showed the comparison of tunneling emission from metal-oxide cathode computed from the exact numerical results and the WKB approximation clear demonstrated the absence of oscillation with the WKB method.[12]

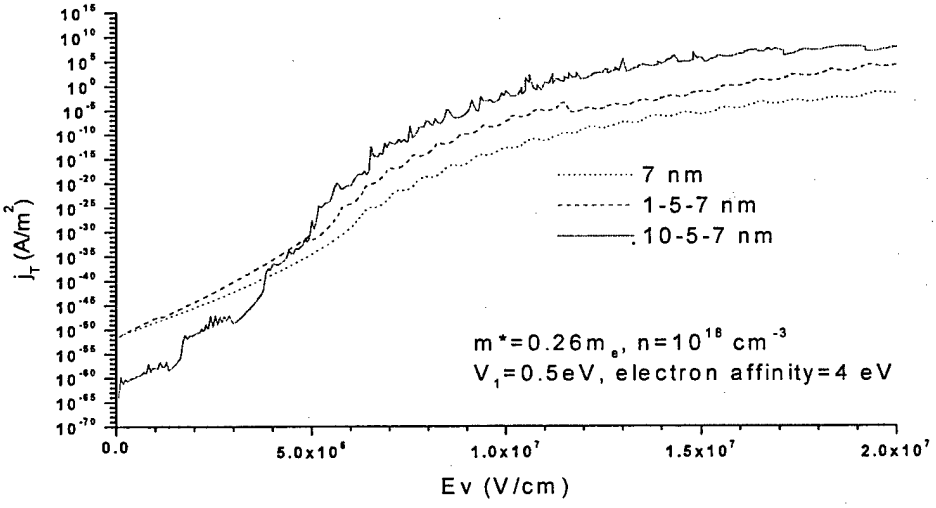

Fig 8 The calculated total tunneling current density vs. the applied electric field for three cases: dotted for the vacuum barrier of 7 nm only, dashed for 1-5-7 nm, and solid for 10-5-7.

Figure 8 shows the calculated tunneling current from Eq. (6). Our results are only valid provided the quantum well region is shorter than the coherence length which is ~ 10 nm, because no scattering is accounted as in the case of including dissipation factors.[13] With a large applied voltage, most part of the barrier moves below the Fermi energy of the contact so that the length we deal with for these resonant states is the sum of the width of the quantum well and a significant part of the barrier width. Earlier we discussed the K-L scheme with a semiconductor step forming a triangular quantum well under a large applied voltage in a material most likely formed by alloying. Alloys are usually poorer in mobility and thus having shorter mean-free-path. Now we have the same problem because our quantum well under a large voltage consists in addition to the quantum well part, a part of the barrier. For this reason, it is far better to have as large a barrier as possible, which cannot be transformed into a quantum well under a large electric field. A wider barrier width but lower barrier height presents extra effective barrier at low field. However, at high field, much of this extra width has a band-edge energy moving below E=0 so that electrons tunneling through the vacuum barrier see a much lowered vacuum level. This is the mechanism for the lowering of the effective work function regardless whether

having resonance or not. Resonance results in additional gain in the tunneling process. To make this extremely important point clearer, we show in Fig. 9 a schematic used for explaining the origin of the large tunneling current at high field – effectively lowering the electron affinity! A bias of +Va is applied in Fig. 9, producing a vacuum electric field of F_o which effectively lowers by $\Delta\phi = F_o(b + w) / \varepsilon$ from ϕ_o. Obviously making b+w large is what lowers the effective ϕ. However if w + b > mean free path of the electrons, the electrons would be near E_c, and no reduction of ϕ_o is possible. Therefore, the additional gain in tunneling results from electrons resonantly tunnel via higher energy levels, the vacuum resonant states above ϕ_o, lowered to the position of the Fermi level in the contact. **In this scheme, the 1st barrier merely serves to keep the high doping in the contact from going into the undoped regions which can be lowered by an applied electric field.** In this respect, the scheme explored by Mumford and Cahay [14] using hot electrons injected from a metal into a wide bandgap semiconductor, resonantly tunnel through a thin semimetal layer to effectively lower the work function bears similar principles.[14] **Only that our present results show that a much simpler scheme for the lowering of the work function is possible: injecting electrons into the quantum well maintaining its energy by avoiding scattering to resonantly tunneling through the quantized vacuum states!**

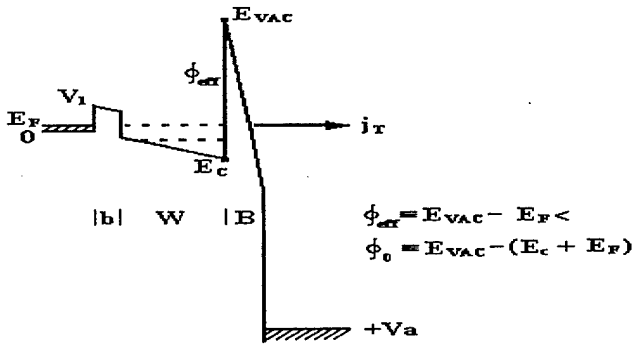

FIG. (9) A schematic potential profile for the DBRT structure under bias of +Va. Note that the work function ϕ_o is reduced by $\Delta\phi$ ~ in the figure.

The computed currents, the total current density j_T, and the hot current density j_H, for 7 nm case, lower trace; and those for 10-5-7 nm, the upper trace, using Si as an example, are shown in Fig. 10. Note that, at a field of ~ 1.5 x 10^7 V/cm, the 10-5-7 case reaches ~ 10^3A/cm^2, which is more than 10^{12} times greater than the case of 7 nm, without the lowering of the effective work function. Therefore our results not only can serve the INE cooling scheme, but also can serve many applications requiring cold cathodes.[15, 16]

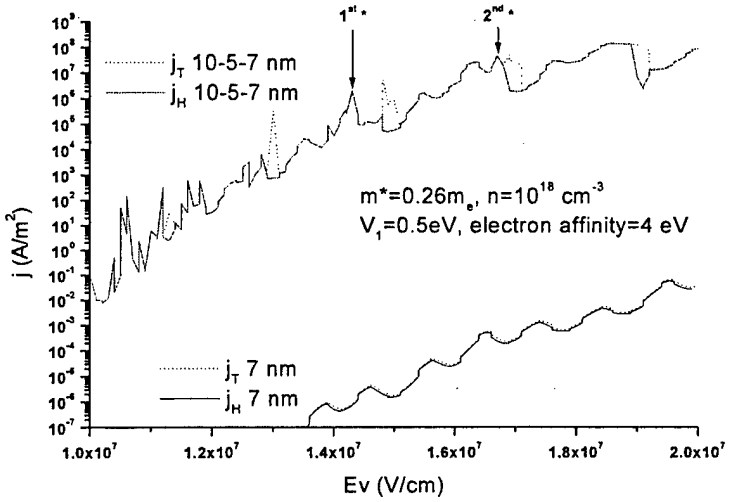

Fig. 10 Computed currents, total current density j_T, and hot current density j_H, for 7 nm case, lower trace; and for 10-5-7 nm, the upper trace, for Si. The two arrows indicate the positions we have calculated the temperature for cooling.

For better visualization, part of the computed results is shown in Fig. 11 with linear scale for the total current densities. The oscillations are much better shown in a linear plot. It is possible to utilize the oscillation for modulation of field emission, for example, turning on and off of a TWT. In fact, these oscillations may be also used to digitize the output of a TWT. It may also be designed with a two-step scheme, one at much lower field for digitization, and amplified by another high power TWT.

A discussion on the placement of the anode is in order. Since barrier-width is reduced by creating a triangular barrier with an applied voltage, as long as the effective barrier width at energy for tunneling is same, it does not matter how far away the anode should be placed. Farther placement of the anode results in more kinetic energy gain after tunneling. Since we assumed that this extra gain in the kinetic energy may be recovered by the Pierce-electrode, we simply place the electrode sufficiently close to reduce computational complexity. In measurements however, it is difficult to design the anode extractor only 7 nm from the front surface.

The barrier height used in our calculation is 0.5eV for silicon may be achieved by epitaxially grown $(Ba_xSr_{1-x})_2 O_3$,[17] as well as recent success in a superlattice structure involving monolayers of oxygen, the Si/O superlattice barrier.[18] Therefore, the calculation using silicon as an example is not just to prove the principle, rather, the structure may be realized. Actually, the III-nitride system seems even more promising because GaN, particularly GaAlN is robust and possibly having low work function. ***To summarize, at a tolerably high electric field, the use of***

resonant tunneling can indeed produce a huge gain in field emission over the case without resonant tunneling even without surface treatment to lower the work function!

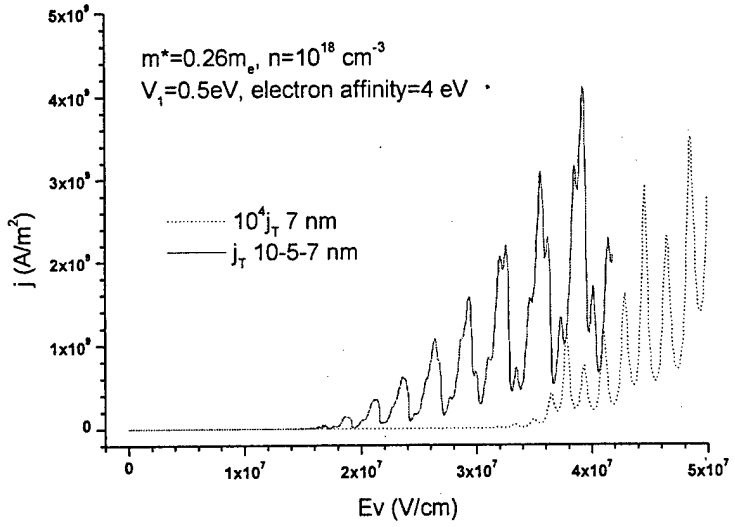

Fig. 12 Oscillations in the resonant tunneling current at high field for two cases.

For practical considerations, we focus our search for the design of getting a relatively high current peak at a field in the low 10^7 V/cm regimes. According to Heinz Busta, formerly of Sarnoff, and Professor Binh of France, a field of $2x10^7$ V/cm may be a practical limit. **Our calculations do show that proper choice of design parameter allows us to keep the electric field at the surface to this limit.**

Calculation of Cooling

For the calculation of the temperature drop from the INE scheme, we start with

$$\nabla \cdot J_Q + \frac{\partial Q}{\partial t} = \Sigma Q, \tag{7}$$

where the right side represents the sum of dissipation – output via emission, explicitly,

$$\Sigma Q = (I^2 R)_{loss} - (J_H V)_{emission}. \tag{8}$$

At steady state and in one dimension, $\frac{\partial Q}{\partial t} = 0$. We assume, for a first order approximation,

$\frac{dT}{dx} \approx 0$, leading to $\frac{dJ_Q}{dx} \approx 0$, or $\Sigma Q = 0$. Without these assumptions, we need to solve the differential equations. In terms of the loss per electron per unit area for the first term in Eq. (2), and the emission term per electron per unit area for the second term in Eq. (2), there results

$$J_T^2 \rho \ell / N_C \exp \{(E_F - E_C) / k_B T\} = J_H V / n, \qquad (9)$$

in which J_T and J_H are the total current, (integration form E = 0 to ∞); and the hot electron current, (integration from $E = E_F$ to ∞), respectively; V is the applied voltage, (anode voltage applied in the vacuum near the surface), ρ is the resistivity of the semiconductor, ℓ is the thickness of the semiconductor, n is the electron density of the semiconductor (The barrier and quantum well are undoped.), and N_C is the effective density of states. Then

$$k_B T = (E - E_F) / \ell n \{ (J_H V / J_T^2 \rho \ell) (N_C / n) \} . \qquad (10)$$

To account for the Wiedemann-Franz law relating the thermal and electrical conductivities, i.e. $K/\sigma = (\pi k_B)^2 T / 3e$, the term $J_H V$ should be reduced to

$$J_Q \cong J_H V - 0.1 k_B T (J_T / e),$$

where J_Q, is the power flow of hot electrons into the vacuum taking into account the Wiedemann-Franz law. Including a thermal load, Eq. (10) becomes

$$k_B T = (E_C - E_F) / \ell n \{ (J_H V / (J_T^2 \rho \ell + \text{Thermal load}) (N_C / n) \} . \qquad (11)$$

At the DARPA HERETIC Principal Investigators' Meeting, Atlanta, GA, on May 23-25, 2001, we have presented the temperature cooling for three materials, Si, GaAs and GaN, in a presentation: [18] "Inverse Nottingham Effect Cooling of Semiconductors With Resonant Tunneling". At that time, we have used a good estimate of the effect of resonance on $\mathbf{J_H}$, from known results of resonant tunneling for contact-to-contact, rather than direct calculation involving putting an anode in the vacuum. Table 1 presented at the HERETIC Meeting is listed below for comparison.

p-type with Inversion : $N_A^- = 10^{18}$ cm^{-3}, C_M (Brown) = 0.013, C_M (Chang-Esaki-Tsu) = 10^{-4}; A^{-1} (Si) = 0.29, A^{-1}(GaAs and GaN) = 0.44

	n_S(cm^{-3})	J_Q (W/cm^2)	J_Q (C)	N_C / n_S	T (K)
Si	**1.8×10^{18}**	**360**	**324**	**22.6**	**296**
GaAs	**4.6×10^{17}**	**1280**	**1042**	**1.02**	**150**
GaN	**3.8×10^{17}**	**1030**	**962**	**6.8**	**187**

n-type : Same values for A^{-1} and C_M as for p-type with inversion

	$n_S(cm^{-3})$	J_Q (W/cm^2)	J_Q (C)	N_C / n_S	T (K)
Si	1.01×10^{18}	325	303	40.3	299
GaAs	2.02×10^{17}	880	843	2.33	138
GaN	0.99×10^{17}	1900	1723	2.6	107

Table 1. Computed Cooling power J_Q for p-type with inversion, and n-type: for Si, GaAs and GaN using an estimation scheme from resonant tunneling from contact-to-contact taken from.[18]

The parameters in the above chart such A^{-1} and C_M is defined in Ref. 2. We compare several cases shown in Table 2 with direct computation. The notations, 1st*, and 2nd*, refer to the points of operation marked by arrows in Fig. 10. For F-N field emission with a single barrier formed by the vacuum level under an applied field at the same operating points. Top chart is for the case without the thermal load. The bottom chart refers to thermal load of 300 W/cm^2. Without thermal load, there is always cooling, even for the F-N case. What it means is that, without thermal load, as long as one takes out the hot electrons, cooling should result, regardless of how low is the current level! This is because we have not included any losses in the calculations. In these charts, NA refers to situation that our theory does not apply or no cooling is possible. The situation is very different when thermal loss is included. With the inclusion of 300 W/cm^2 of thermal load, F-N emission cannot cool because the remover of power via field emission is less than the thermal load. What is interesting is the fact that there is an optimum cooling. Going from the 1st to 2nd, while P_H is much increased, but cooling is reduced because the loss due to current flowing through the substrate is even higher. We shall also compare the results for P_H obtained previously with the present direct calculation: Previously, P_H = 325 W/cm^2 while the direct calculation gives 2442 W/cm^2. **What is most encouraging is the fact that a cooling of 103 K is still possible with 300 W/cm^2 of thermal load, employing resonant tunneling operating at an electric field ~ 1.5x10^7 V/cm, which is manageable in practice.**

Without Thermal Load

		P_L (W/cm^2)	P_H (W/cm^2)	T (K)	ΔT (K)
Resonance	1st *	40	2442	143	157
	2nd *	22563	67450	233	67
Without Resonance	1st *	6.29×10^{-24}	6.62×10^{-11}	33	267
	2nd *	9.80×10^{-19}	8.38×10^{-8}	39	261

With 300 W/cm^2 of Thermal Load

		P_L (W/cm^2)	P_H (W/cm^2)	T (K)	ΔT (K)
Resonance	1st *	340	2442	197	103
	2nd *	22863	67450	233	67
Without Resonance	1st *	300	6.62×10^{-11}	NA	NA
	2nd *	300	8.38×10^{-8}	NA	NA

Table 2. Results of direct computation for tunneling into the vacuum

The term P_L refers to the contribution of loss from $J_T^2 \rho \ell$, which is quite negligible compared to the thermal load used at the operating point 1st, however, the loss is huge at the 2nd operating point. The term P_H refers to the rate of energy removed via field emission of the hot electrons above the Fermi level.

Discussion

Our calculated results show that INE can be realized. What is exciting is the fact that resonant tunneling into the vacuum gives ~10^{3-4} times higher emission current over the case without resonance at an electric field quite manageable. Even if INE cooling scheme is ultimately proved to be impractical due to the difficulty with the Pierce-electrode, the huge gain in the emission current should have a strong impact in cold cathode vacuum electronic devices. Since the DBRT structure is planar, it should be much more robust than geometrical structuring.

As pointed out before, the low field emission reported by Binh and Adessi, [20] require further discussion. First of all, inserting TiO_2 between the metal and the vacuum, structurally their scheme is similar to the K-L scheme shown in Fig. 2. The calculation in the K-L scheme is based on resonant tunneling, which takes into account the quantized sub-bands in the well created by the applied high electric field. However, if losses and dampings are high, quantized sub-bands cannot exist so that the two models are structurally identical. The question remains why Binh and Adessi measured low emission current at such low electric field. Heinz Busta thought that the low current field emission comes from defects inadvertently introduced. It is likely that the high dielectric TiO_2 results in "smoothing" the localized defects rendering the appearance of more uniform emission. We have calculated the K-L scheme from Eq. 6 using the same parameters as in Ref. 3. The total current density is compared with our model as well as the F-N case without resonant tunneling in Fig. 13. Note that the high emission occurs at a field of over 3×10^7 V/cm. As we have pointed out before that usually the mobility of a step using

alloying is much reduced so that losses should be included. Nevertheless, it is impressive that such a simple structure with a step is capable of producing a current less than a factor of ten below the DBRT case!

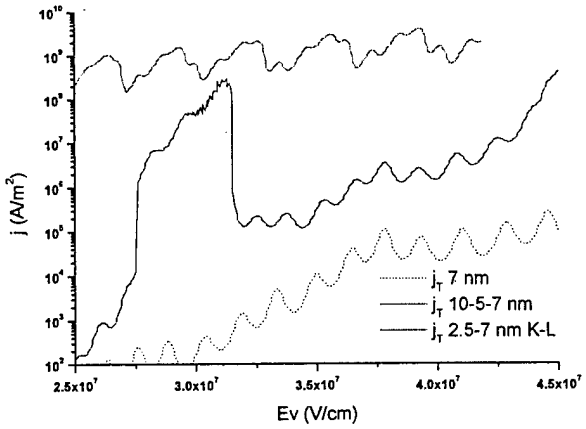

Fig.13 Comparison of the total tunneling current density between the K-L scheme, our DBRT case, with the F-N case without resonant tunneling.

The large gain in the tunneling current compared to the case without shown in dotted is again due to the lowering of the effective work-function. The additional gain between 2.75 – 3.3 x 10^7 V/cm is due to resonance gain. We have computed several cases for GaN – AlGaN-GaN system, seems to be the best possible choice for high current emission discussed previously. Figure 14 gives the calculated total current density vs. electric field in the vacuum for GaN-$Al_{0.5}Ga_{0.5}N$-GaN with b/w/B cases as shown. A single vacuum barrier of 2nm is also shown for comparison. The effective mass for the barrier and quantum well are taken to be 0.22 m_0 and the barrier height is taken to be 0.8 eV. The internal build-in field, ~ 2-3.6 x 10^6 V/cm, has not been included. The calculated current density near a field of 1.5 X 10^7 V/cm is 10^4 A/cm^2. Considering the robustness of the III-nitride system, this is the best choice thus far. In fact we predict that the ideal emitter may be achieved by adding a second barrier of few monolayers of AlN at the surface of GaN both as a protection against oxidation as well as for further lowering the effective work function. **Such a system cooperating at a reduced temperature (The field emitter will be self-cooled by the INE cooling process.) will be an ideal cold cathode for TWT and other applications requiring high current protected from oxidation of the emitter.**

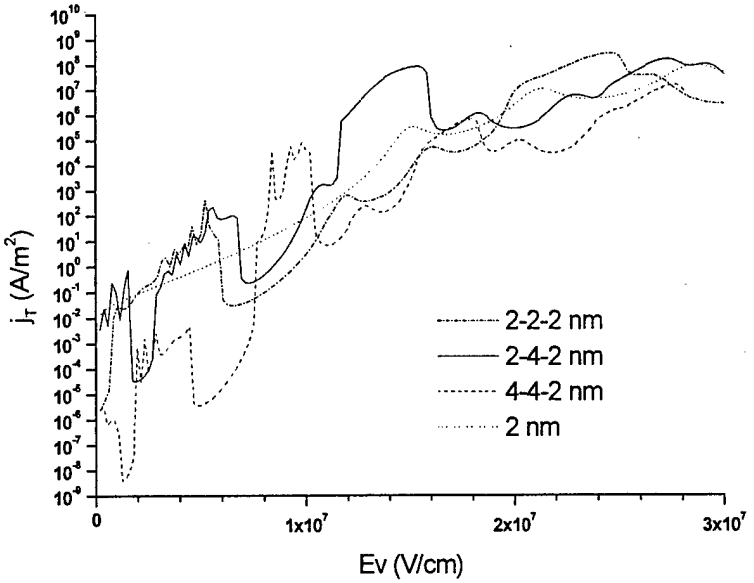

Fig. 14 Calculated total Current Density vs. Electric Field in the vacuum for GaN-$Al_{0.5}Ga_{0.5}N$-GaN with b/w/B cases as shown. A single vacuum barrier of 2nm is also shown for comparison. The effective masses for the barrier and quantum well are taken to be 0.22 and the barrier height is taken to be 0.8 eV. The internal build-in field, ~ 2-3.6 x 10^6 V/cm, has not been included.

Conclusion

Let us discuss what is universally known in the field emission community. Most researchers agree that for a field > 2x10^7 V/cm, the usual Fowler-Nordheim emission would result in substantial emission current. At a significantly lower field, work-function lowering such as Ce on Si so that usuful emission can take place much below 1x10^7 V/cm, for avoiding surface degradation. Our samples measured by Heinz Busta at Sarnoff, as well as the samples from KL method designed by Kostantin K. Likharev and fabricated by Wiley P. Kirk (Texas A & M University) using ZnS on Si and measured by Vu Thien Binh (Laboratoire d'Emission Electronique, Département de Physique des Matériaux, UMR-CNRS, Université Claude Bernard Lyon 1) showed structure in emission current at field of ~1x10^6 V/cm or lower, which may be caused by some inadvertently introduced surface contaminants. What we know now is the fact that the main factor in obtaining significant emission current at relatively low applied electric field still needs low work-function at the surface. Since work function lowering has been an intensive research for more than 30 years, we want to see whether it is possible to design field emission via resonant tunneling without work function lowering, capable of producing substantial emission at an electric field below 1x10^7 V/cm. We are reassured that calculations

show that it is indeed possible! Resonant tunneling not only can improve transmission by a mechanism similar to photon resonance cavity, the appearance of higher energy sates due to quantum confinement effectively lowers the work function at the semiconductor vacuum interface. Even if INE cooling would be too difficult practically, the huge increase in the tunneling current into the vacuum would open the door for vacuum electronics with efficient cold cathode. Recently, we have fabricated two samples, one with Si and a second one with GaN for measurements in V.T. Binh's laboratory in France. Preliminary results indicated that the huge enhancement in the resonant tunneling current into the vacuum is close to predicted value.[21]

References

1. W.B.Nottingham, *Phys. Rev.* **59** (1941) 908-907
2. R. Tsu and R.F.Greene, "Inverse Nottingham Effest Cooling in Semiconductors", *Electrochem and Solid-State Lett.,* **2** (1999) 645-647 (1999)
3. R.F.Greene and R. Tsu, *Workshop on Microelectronic Thermal Management, System Planning Corporation*, DARPA ETO, E.Towe and E.Brown, Arlington, VA, Dec.11- 12, 1997
4. A. Korotkov and K. Likharev, *Appl. Phys. Lett.* **75** (1999) 2491-2493
5. R. Tsu and L. Esaki, *Appl. Phys.Lett.* **22**, (1973) 562-564
6. L.L.Chang, L.Esaki and R. Tsu, *Appl. Phys. Lett.* **24** (1974) 593-595
7. R. Tsu, *ECS Proc.* **98-19** (1999) 3-16
8. A.S.Gilmore Jr., *Microwave Tubes*, (Artech House Inc. 1986)
9. Y. Yamaoka, S. Kanemaru, and J. Itoh, *J. Appl. Phys.* **35** (1996) 6626-6628
10. D.D.Coon and H.C. Liu, *Appl Phys.Lett.* **47** (1985) 172-174
11. Optical Properties of Quantum Steps, H. Shen, F. H. Pollak and R. Tsu, *Appl. Phys. Lett.* **57** (1990) 13-15
12. H. Mimura, Y. Abe, J. Ikeda, K. Tahara, Y. Neo, H. Shimawaki, and K. Yokoo, *J.Vac.Sci. Technol.* **B16 (2)** (1998) 803-846
13. R. Tsu, *J. Non- Crystalline Solids* **114** (1989) 708-710
14. P.D. Mumford and M. Cahay, *J. Appl. Phys.* **79** (1996) 2176-2179
15. I. Brodie and C.A. Spindt, *Adv. Electro. Electron Phys.* **83** (1992) 1-106
16. S. Iannazzo, *Solid-state Electron* **36** (1993) 30-320
17. Private communication from William Shelton of Oakridge National Lab.
18. R. Tsu, A. Filios, C. Lofgren, K. Dovidenko and C.G. Wang, *Electrochem and Solid State Lett.***1** (1998) 80-82
19. R.Tsu and R.F.Greene, *DARPA HERETIC Principal Investigators' Meeting,* Atlanta, GA, May 23-25, 2001.
20. V.T. Binh and C. Adessi, *Phys. Rev. Lett.* **85** (2000) 864-867
21. V. Semet, V.Binh, J, Zhang, J.Yang, A.Khan and R. Tsu, Electron emission through a multilayer planar nanostructured Solid-state field-controlled emitter, Appl. Phys. Lett. **84**, 1937 (2004)

(4) No Patent filed

Unexpected Dividend

The success of the cooling scheme depends on how successful to pull electrons from the semiconductor to the vacuum. What is most satisfying was a phone call I received from Professor Binh that something is wrong with the sample and calculation, that the measured exceeded the calculated by a large factor! I immediately realized that the work function at the surface has been further lowered by the space charge occupying the quantum states. However, there is no way to get the field low enough to match the measured unless we assume that the electron occupying the ground state of the quantum well has actually moved below the Fermi level at the contact so that the sub-bend is fully occupied, resulting in a large space charge as shown in the figure below. We solved the system self-consistently and found that the effective work function is further lowered by almost 1eV!

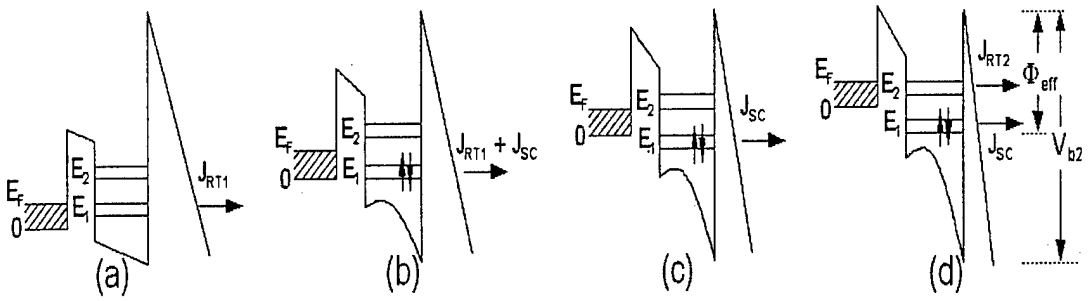

Figure: Illustration of the different field emission mechanisms by a schematic band edge diagrams of the nanostructured SSE planar cathode with an applied field F and at room temperature. (a) only resonant tunneling mechanism; (b) to (d) evolution with space charge formation inside the GaN layer with, as consequence, an effective lowering of the surface barrier. In addition to the resonant tunneling and due to the occupation of the quantum state E_1, electrons occupying this state (for example, whenever the level E_1 moves below 0) can tunnel out of this single barrier via the usual F-N tunneling, resulting in J_{SC} (Fig. 3c), and the total current $J_{FN} = (J_{RT} + J_{SC})$. (Notes: (i) to be able to present these band diagrams within this figure, the field representation is not at the same scale inside the cathode and outside in vacuum in particular if one considers GaN having $\varepsilon = 8\varepsilon_o$ with an applied field in the range of 50 V/μm; (ii) further reduction from the induced image charges due to the space charge in the quantum well is not shown in this sketch).

This happy ending was not anticipated. In retrospect, one may ask why no one predicted that. What is surprising is the fact that I started the resonant tunneling work more than 30 years ago, and I failed to predict this result. In summary, now we know that the best way to bring down the work function is to use a quantum well structure on the surface of a semiconductor to create quantum states boxed in by the vacuum level and a barrier. At some appropriate field, the space charge is shifted up due to the presence of the quantum states which are brought near the vacuum level. Obviously due to quantum confinement, there is a slowing down of the process due to resonant effects. However, a typical RTD is capable of operating near THz, even with a resonant system having a Q = 100, we are still talking about 10 GHz time-response. As a cold cathode, it should be fast enough to modulate emission at 10GHz!

Now I would like to attache the reprint of the recent publication in Appl. Phys. Lett. **84,**1937 (2004)

APPLIED PHYSICS LETTERS VOLUME 84, NUMBER 11 15 MARCH 2004

Electron emission through a multilayer planar nanostructured solid-state field-controlled emitter

V. Semet and Vu Thien Binh[a)]
Equipe Emission Electronique, LPMCN-CNRS, University of Lyon 1, Villeurbanne, 69622, France

J. P. Zhang, J. Yang, and M. Asif Khan
Department of Electrical Engineering, University of South Carolina, Columbia, South Carolina 29208

R. Tsu
Electrical and Computer Engineering, University of North Carolina at Charlotte, Charlotte, North Carolina 28223

(Received 21 October 2003; accepted 21 January 2004)

We have measured the field electron emission (FE) from a surface covered with two ultrathin layers of semiconductor, 4 nm GaN on 2 nm $Al_{0.5}Ga_{0.5}N$. The threshold field was 50 V/μm, with stable FE current densities up to 3×10^{-2} A/cm^2. We have also measured the FE dependence with field and temperature and determine then an effective surface tunneling barrier ≈0.5 eV, coexisting with an effective thermal activation energy of ~0.85 eV. To interpret these experimental results, we propose a dual-barrier model, related to the nanostructured layers, with a serial two-step mechanism for the electron emission, taking into account the space charge formation in the quantum well structure at the surface. © *2004 American Institute of Physics*. [DOI: 10.1063/1.1682701]

Field electron emission requiring low electric field represents a big challenge for applications running from the realization of field emission planar structures through local cooling by using inverse Nottingham effect[1–3] without surface structuring such as sharp tips or ridges. An approach by modifying the electronic properties of the underneath surface layer, called solid-state field-controlled emission (SSE), has been recently proposed.[4] In this letter, we present the first experimental measurements of electron emission from multilayer nanostructured SSE cold cathodes. By introducing the multilayer concept, we introduce more parameters for the control of the SSE process, such as the bulk interfacial barrier in addition to the surface barrier and the presence of quantized subbands due to the confine thickness of the outmost layer. Specific electron emission has been measured from these cathodes. A new model based on a dual barrier mechanism for electron emission through the nanostructured layers is proposed from the interpretation of the experimental data.

We show the actual structure of the cathode in Fig. 1(b). The structure was deposited on *n*-SiC using low-pressure metalorganic chemical vapor deposition. Trimethylaluminum, trimethylgallium, silane, and NH_3 were used as the precursors. First, a 0.15-μm-thick Si-doped AlGaN layer with Al-content graded from 40% to 15% was deposited on the SiC substrate. It served as the conducting buffer layer. This was followed by 0.25 μm *n*-GaN, 2 nm *n*-$Al_{0.5}Ga_{0.5}N$ and 4 nm undoped GaN. The Si-doping level in all the doped layers was about 2×10^{18} cm^{-3}, and the finished surface was characterized to be atomically smooth by atomic force microscope over the whole surface of the cathode having a total area of about 2 cm^2.

The band edge diagram of this nanostructured layer cathode [Fig. 1(a)] presented then a confine layer of 4 nm limited by a first barrier $F_{b1}=0.8$ eV at the interface of GaN with $Al_{0.5}Ga_{0.5}N$ and a second barrier $F_{b2}=1.5$ eV at the cathode surface of GaN with vacuum, in the absence of applied electric field.

Let us first present the experimental measurements. The $I-V$ measurements were performed with a piezo-driven scanning anode field emission microscope [(SAFEM)—Fig. 1(b)].[5] The whole set of data ($I-V$) obtained for different values of z (insert in Fig. 2) were analyzed using electron optics numerical simulations (this analysis was detailed in Ref. 5) in order to have, for each location at the surface cathode and a given temperature, an unique $J_{emi}-F$ plot

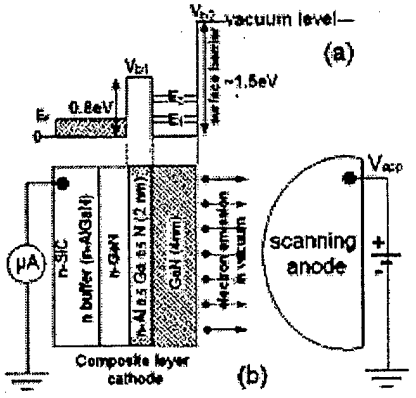

FIG. 1. Nanostructured layers of the cold cathode. (a) Band edge diagram in the absence of an external electric field ($V_{app}=0$); F_{b1} and F_{b2} are, respectively, the first and second barriers; E_1, E_2 are the energy levels of subbands inside the quantum well. (b) Schematic structure of the different layers of the cathode within the SAFEM environment.

a)Author to whom correspondence should be addressed; electronic mail: vuthien@lpmcn.univ-lyon1.fr

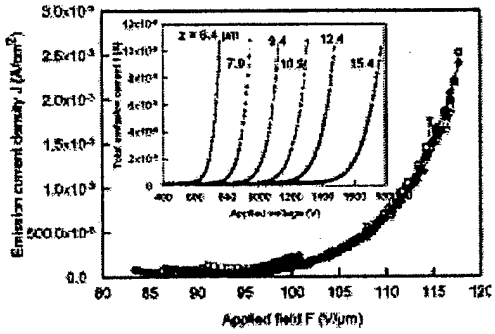

FIG. 2. Emission current density J_{meas} vs the actual field F at the surface of the nanostructured SSE cathode at 160 °C, i.e., in the presence of a thermionic like emission [see the discussion of characteristic 2 in the text]. In the insert are the plots of the total emission current I vs applied voltage V_{appl}, for six different distances z between the anode and the cathode. The convergence of all the I–V data toward a unique J_{meas}–F plot for different z values was a confirmation of the correctness of the emission measurements and analysis (Ref. 5). From these data, plotting $\ln(J_{meas}/F^2)$ vs $1/F$ gave a straight line, which means a FN behavior for the emission characteristics.

(Fig. 2). J_{meas} is then the measured emission current density and F is the related real field at the surface of the planar cathode. The (J_{meas},F) values obtained could then be compared directly with theoretical values used in the different analytical approaches.

We have done measurements for different locations across the cathode and for different temperatures. The emission characteristics presented in the following were common to all these measurements and can then be considered as specific to this nanostructured SSE.

(1) For a given temperature, the $(J_{meas}$–$F)$ evolution presented the following three main characteristics: (i) The threshold field for $J_{meas}=10^{-4}$ A/cm^2 was in the range of 5×10^5–1×10^6 V/cm at room temperature. This value is about 100 to 50 times less than the conventional field needed for field emission from a metallic surface with a work function of about 4 eV. (ii) The $\ln(J_{meas}/F^2)$ vs $(1/F)$ plots of the data were straight lines, i.e., the increase of the field emission (FE) current can be described on the basis of electron tunneling through a barrier deformed by high external electric field known as the Fowler–Nordheim (FN) theory.[6,7] The deduced experimental values of the tunneling barrier height Φ_{FN} were in the range of 0.25–0.5 eV for the different locations. There was no dependence of Φ_{FN} with temperature. (iii) We always noted a very brutal and sharp increase of the emitted current in the high field region and for $J_{meas}\geqslant3\times10^{-2}$ A/cm^2. This sharp increase ended, in most cases, with the destruction of the surface cathode due to an arc formation between the cathode and the anode.

(2) Emission currents were very unstable at the beginning of the emission process. These instabilities always slowly vanished after a conditioning period of more than 1/2 h of continuous emission of the cathode at high currents. After the healing of the instabilities, the emission currents became very stable. We have observed these instabilities for all cathode temperatures up to 500 K. It seems then that they were intrinsic to the emission mechanism and were not the result of a surface absorption–desorption process that will modify the emission.

(3) For a given emission area, the emission currents increased with temperature from 300 to 500 K. As this behavior cannot be explained by the FN theory, we have used the Richardson–Dushman approach[8] to determine the effective thermal activation energy related to these data. The deduced values from the experimental data were in the range of 0.8–0.9 eV and they were not field dependent.

Let us point out the two characteristics of the field emission from the nanostructured SSE cathode surface: (i) The values of the tunneling barrier height Φ_{FN} were in the range of 0.25–0.5 eV, this value has to be compared with the 1.5 eV value of electron affinity of GaN. (ii) This value is much smaller than the thermal activation energy Q (0.8–0.9 eV) obtained from the temperature dependence emission. This means that the tunneling barrier at the surface is not the thermionic barrier. Note that Q is very near the height of the barrier between the buffer layer and $Al_{0.3}Ga_{0.7}N$ layer (Fig. 1).

To account for this specific electron emission from the nanostructured SSE we propose the following model, schematically described in Fig. 3. In this model the electron emission is obtained through a serial two-step mechanism under applied field, similar to the one in Ref. 4. In a first step, electrons are injected in the GaN layer from the cathode substrate by tunneling through the 2 nm $Al_{0.3}Ga_{0.7}N$ layer. They will occupy the subbands that are under the Fermi level, creating a concentration of electrons inside the GaN layer. Due to this electron concentration or space charge formation, there is an upward energy shift, which is schemati-

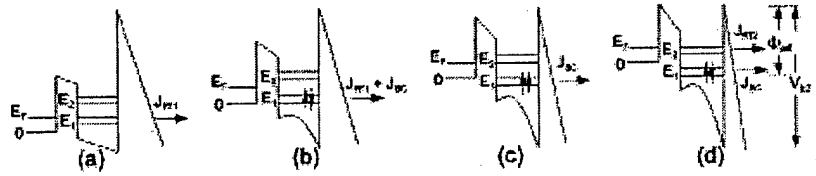

FIG. 3. Illustration of the different field emission mechanisms by schematic band edge diagrams of the nanostructured SSE planar cathode with an applied field F and at room temperature: (a) only resonant tunneling mechanism; (b)–(d) evolution with space charge formation inside the GaN layer with, as a consequence, an effective lowering of the surface barrier. In addition to the resonant tunneling and due to the occupation of the quantum state E_1, electrons occupying this state (for example, whenever the level E_1 moves below 0) can tunnel out of this single barrier via the usual FN tunneling, resulting in J_{SC} [Fig. 3(c)], and the total current $J_{FE}=(J_{RT}+J_{SC})$. [Notes: (i) To be able to fit these band diagrams within this figure, the field representation is not at the same scale inside the cathode and outside in vacuum, in particular if one considers GaN having $\varepsilon=8\varepsilon_0$ with an applied field in the range of 50 V/µm; (ii) further reduction from the induced image charges due to the space charge in the quantum well is not shown in this sketch].

cally represented in Fig. 3 with the evolution from (b) to (d); leading to a relative lowering of the vacuum level compared to the Fermi level of the substrate.

In this model, the two concomitant mechanisms for the electron emission are described hereafter in (A) and (B):

(A) The first mechanism is the tunneling field emission through a lowering work function, i.e., the electrons are emitted by a field emission mechanism from the quantized subbands inside the GaN quantum well.

Figure 1(a) shows two quantum well (QW) states E_1 and E_2 at a bias voltage $V=0$. In the conventional resonant tunneling approach,[6,9,10] with the application of a bias at $V=V_1$, the state E_1 is aligned with the electrons in the contact at energy $0<E<E_F$, resulting in a resonant tunneling current, J_{RT1} [Fig. 3(a)]. There is then a small lowering of the effective work function. However, this lowering by itself is not enough to allow electron emission by tunneling with fields in the range of 10^5-10^6 V/cm,[10] and also it cannot account for the very low values of Φ_{FN}, the measured tunneling barrier of the nanostructured SSE.

In our two-step tunneling model, a larger lowering of the work function due to space charge in the QW is crucial. The concept is when this two-dimensional (2D)-like quantum state is occupied it results in a space charge in the QW, leading to additional lowering of the effective work function defined by the energy of the source of electron to the vacuum level. A precise quantitative approach requires the use of the Airy function when a voltage is applied to the structure, with self-consistent calculations.[4,11] However, to estimate the lowering of the work function here we used a simpler approach, involving first finding the potential due to the space charge inside the 2D quantum well. Using this calculated lowering of the work function, the usual field emission expression derived from the FN theory is then fitted to the experimentally measured field emission.

In the QW of width w, assuming a perfect confinement, the charge density in the lowest level E_1 is $n=e(m^*/\pi\hbar^2)\times(E_2-E_1)(2/w)\sin^2(\pi x/w)$, where m^* is the effective mass of the electron with charge e. Solving the Poisson's equation we arrive at the potential energy of the space charge V_{SC}, for $0\leq x\leq w$,

$$V_{SC}=(\rho_0/4\varepsilon)\{(w/\pi)^2\sin^2(\pi x/w)+wx-x^2\}, \qquad (1)$$

where $\rho_0=e(m^*/\pi\hbar^2)(E_2-E_1)(2/w)$ and ε is the dielectric constant.

The maximum value of V_{SC} is at $x=w/2$, $V_{SC}[w/2]=(0.25\,\rho_0/\varepsilon)w^2\times(\pi^{-2}+0.25)$, and the average of V_{SC} is $V_{SC}[\mathrm{av}]=0.62\times V_{SC}[w/2]$. Taking the average of the difference $[V(w)-V(0)]$, the total lowering of the work-function $\Delta\Phi=V_{b2}-\Phi_{eff}$ is

$$\Delta\Phi=V_{SC}[\mathrm{av}]+0.5\times[V(w)-V(0)]+E_1. \qquad (2)$$

The effective barrier Φ_{eff} is the actual barrier at the surface after the lowering and can be determined experimentally from the (J_{max},F) plots, i.e., Φ_{FN}.

For an estimation of $\Delta\Phi$ we have taken $m^*=0.22m_0$, $\varepsilon=8\varepsilon_0$ for GaN, $V_{SC}[w/2]=0.4$ eV, $0.5\times[V(w)-V(0)]=0.62$ eV, and $E_1=0.18$ eV. This gives $\Delta\Phi=1.05$ eV, i.e., $\Phi_{eff}=0.45$ eV for $V_{b2}=1.5$ eV. This calculated value 0.45 eV for the effective surface barrier is very near the experimental values Φ_{FN} measured from the (J_{max},F) plots, which were in the range of 0.25–0.53 eV.

Therefore, we conclude that after the occupation of the quantum level for the electron in the state E_1 lying below $E=0$, the tunneling current $J_{FN}=J_{RT}+J_{SC}$ is given by the FN tunneling through a single barrier created by the vacuum, with an effective barrier of only a few tenths an electron volt [Fig. 3(d)]. This lowered barrier at the surface controls the variation of the emitted current J_{FN} with field.

(B) The second mechanism occurs for elevated temperatures, i.e., $k_BT>0.8$ eV, when hot electrons can jump over the first barrier located between the conductive substrate and the $Al_{0.5}Ga_{0.5}N$ ultrathin layer. As the second barrier at the surface is lower (less than 0.5 eV due to space charge) these electrons will emit directly, given J_{TH}. This first barrier controls the variation of the emitted current J_{TH} with temperature.

In this dual-barrier model, the measured total emission current, J_{max}, will be the sum of both contributions, $J_{max}=J_{FN}+J_{TH}$. Note that we have made numerical simulations in order to confirm that in our case by using J_{max} we can calculate with good accuracy either Φ_{FN} or Q by using, respectively, the plots $\ln(J_{max}/F^2)$ versus $(1/F)$ and $\ln(J_{max}/T^2)$ versus $(1/T)$.

In conclusion, we have shown in this letter that a nanostructured SSE planar cathode gives the possibility to control the effective surface barrier for electron emission by monitoring the space charge value of an ultrathin layer at the surface. Compared to a one-layer SSE,[4,12] by using a multilayer nanostructured SSE we have added the possibility for a fine control of the space charge value with the presence of subbands in the QW. Moreover, the presence of the first barrier induces a separation between the thermionic process from the field emission process which is controlled by the second barrier at the surface. This last possibility must enforce, for example, the control of the cooling process by inverse Nottingham process.[10]

R.T. would like to acknowledge DARPA/ARO HERETIC program for the support of this research.

[1] W. B. Nottingham, Phys. Rev. **59**, 906 (1941).
[2] A. Korotkov and K. Likharev, Appl. Phys. Lett. **75**, 2491 (1999).
[3] R. Tsu, Proc. Electrochem. Soc. 2000-28, 91 (2001).
[4] V. T. Binh and Ch. Adessi, Phys. Rev. Lett. **85**, 864 (2000).
[5] V. T. Binh, V. Semet, J. P. Dupin, and D. Guillot, J. Vac. Sci. Technol. B **19**, 1044 (2001).
[6] R. Tsu and L. Esaki, Appl. Phys. Lett. **22**, 562 (1973).
[7] J. W. Gadzuk and E. W. Plummer, Rev. Mod. Phys. **45**, 487 (1973).
[8] A. Reimann, *Thermionic Emission*, (Wiley, New York, 1934).
[9] L. Esaki, Rev. Mod. Phys. **46**, 237 (1974).
[10] Y. Yu, R. F. Greene, and R. Tsu, in *Advanced Semiconductor Heterostructures*, edited by M. Dutta and M. A. Stroscio (World Scientific, New Jersey, 2003), Vol. 28, pp. 145–162, also in Int. J. High Speed Electron. Syst. **12**, 1083 (2002).
[11] K. L. Jensen and A. K. Ganguly, J. Vac. Sci. Technol. B **12**, 770 (1994).
[12] V. T. Binh, Appl. Phys. Lett. **78**, 2799 (2001).